Available online at www.sciencedirect.com
SCIENCE DIRECT®
Polymer 44 (2003) 3661–3670
polymer
www.elsevier.com/locate/polymer

Probing the interface behaviour of injection molded thermoplastics by micro-thermal analysis and temperature-modulated differential scanning calorimetry

S.A. Edwards, M. Provatas, M. Ginic-Markovic, N.Roy Choudhury*

Ian Wark Research Institute, University of South Australia, Mawson Lakes BLVD., SA 5095, Australia

Received 26 September 2002; received in revised form 3 March 2003; accepted 2 April 2003

Abstract

Micro-thermal analysis (μTA™) and temperature-modulated differential scanning calorimetry (TMDSC) are emerging as powerful instruments for identifying the existence and quantities of phases in multi-component systems, as well as interfacial properties. In this study, these two complimentary techniques are utilised to probe the interphase behaviour of a polycarbonate/acrylonitrile–styrene–acrylate (PC/ASA) blend as they develop during injection molding. Micro-thermal analysis revealed that parts manufactured at high injection time, pack pressure and melt temperature show a densely packed bulk morphology, a significant amount of particle agglomeration as well as the formation of styrene–acrylonitrile/PC (SAN/PC) interphases. TMDSC qualitatively and quantitatively characterized the PC/ASA's multi-phase morphology and its interfacial properties both before and after injection molding, indicating a greater amount of PC entering the interphase than SAN.

Keywords: Interfaces; Micro-thermal analysis; TMDSC

1. Introduction

Modern thermoplastic materials are usually blends or composites of complex morphologies that determine their intrinsic properties. The performance of any complex material is mainly controlled by its component suprastructure design and properties or morphology. Polymer morphology thus deals with the arrangement of polymer molecules into amorphous or crystalline regions, the form and structure of these regions and the manner in which they are organised into more complex units. Morphology of a multi-component system or blend defines the spatial arrangement of the component phases [1].

Modern thermal analysis techniques such as micro-thermal analysis and temperature-modulated differential scanning calorimetry (TMDSC) are emerging as powerful tools for identifying the existence and quantities of phases in multi-component systems [2–4], as well as the properties of interfaces between phases [1,5–7]. Micro-thermal analysis is a unique tool that combines the capabilities of advanced thermal analysis with atomic force microscopy (AFM) [8–14], closely examining the surface and near-surface layers of substrates, correlating physical properties and topography with observed phases and boundary layers [15]. Furthermore, by applying a heating signal on a small area of the solid substrate, it is possible to perform localised thermal analysis (LTA) in highly focused areas of interest on the sample to obtain data such as glass transition (T_g), crystallization and melting temperatures [16].

Although various microscopic methods [1] have been used to characterize the morphology of acrylonitrile–butadiene–styrene (ABS) and PC/ABS blends, the application of micro-thermal analysis to the characterization of interphases developed while processing blends such as polycarbonate/acrylonitrile–styrene–acrylate (PC/ASA) has not yet been reported. The current state of knowledge of this instrument is in its early stages and thus few references are available outlining the principle and modes of its operation. To date, most studies conducted using micro-thermal analysis have been applied in the realm of pharmaceutical chemistry [17] and biological sciences [18–20]. In our previous work [6] we reported the use of micro-thermal analysis in characterising the in situ developed multi-phase morphology of engineered surface defects on ideal and non-ideal PC/ASA parts. When such a rubber-modified polymer melt cools and solidifies, it forms a gradient in molecular packing and hence density. In general,

* Corresponding author. Tel.: +61-8-8302-3719; fax: +61-8-8302-3755.
E-mail address: namita.choudhury@unisa.edu.au (N.R. Choudhury).

0032-3861/03/$ - see front matter © 2003 Elsevier Science Ltd. All rights reserved.
doi:10.1016/S0032-3861(03)00291-X

an amorphous surface region is formed and the bulk phase becomes the core. Fractions not accommodated in that core morphology are rejected to the surface. This can occur due to either incompatibility of the two phases, lower molecular weight and hence viscosity of one or more components, or to the mismatch of their surface energy. However, if the melt is cooled and solidified against a nucleating surface, such as a high-energy mold, a surface having a significant variation in density results. Thus, during injection molding of PC/ASA, a preferential phase segregation mechanism produces a highly orientated PC-skin layer on the surface with the amount of ASA increasing towards bulk regions [1,21].

While micro-thermal analysis visualizes and characterizes the morphology of such rubber-modified plastics, further quantitative information on multi-component polymers and polymer blends is still required. In practice, direct measurements of free energy of mixing, interaction parameters, etc. are difficult and therefore miscibility is often judged by the degree of dispersion, for example, the size of the phases. A variety of microscopic, thermal, and calorimetric methods can be used to determine size of the phases. For example, transmission electron microscopy (TEM) can be used to analyse domain size, domain distribution and phase continuity down to a resolution of 1 nm. However, a combination of various methods is often used for a better understanding of blend miscibility.

Accurate measurements of glass transition temperature by DSC is a useful technique for investigating the interfacial properties of polymer blends. In such materials, the basic limitations is the determination of T_g with components that have similar or close values ($<15\,^{\circ}C$ difference), where resolution of T_g by conventional calorimetric or dynamic mechanical methods becomes impossible. Also for small concentrations ($<10\%$), the transition signal is weak and difficult to resolve. TMDSC provides not only the same information as conventional DSC but also provides unique information by overcoming most of these limitations, characterising interfacial behaviour and miscibility with high resolution.

By superimposing a sine wave on the conventional DSC heating ramp, TMDSC can provide a response in two functions: the heat capacity (C_p) and the total heat flow [22–25]. The heat capacity is a continuous function that is sensitive to the glass transition process. The value of this parameter can be detected by TMDSC in the glass transition region, independent of any enthalpic events that may otherwise make its interpretation more difficult. By accurately measuring the increment of the heat capacity signal at the glass transition temperature, the interfacial properties of multi-phase systems can be interpreted. These properties can include the extent of mixing, phase separation, weight fraction at the interface and the extent of inter-diffusion [26–30].

The blending of two dissimilar polymers has often been monitored by observing the change in the T_g region. Studies by Song et al. [28] have shown that for blends showing a significant degree of interface development, the increment of heat capacity, ΔC_p at T_g, is smaller for both polymers than those of their physical blends. However, between their glass transition temperatures, the values of dC_p/dT signals of the blends are larger than the corresponding physical blends, indicating the formation of an interphase. For an immiscible, multi-phase polymer system, the total ΔC_p is given as the sum of the ΔC_p of its pure components using the following expression [27]

$$\Delta C_p = \omega_{10}\Delta C_{p10} + \omega_{20}\Delta C_{p20} \tag{1}$$

where ω_{10} and ω_{20} are the weight fractions of polymer 1 and polymer 2, respectively, in the 2-phase, immiscible blend and ΔC_{p10} and ΔC_{p20} are the heat capacity increments at each polymer's corresponding T_g's before mixing. Studies have shown [26,30,31] that the values of ΔC_{p10} and ΔC_{p20} vary when the proportion of constituents are changed. This has been postulated to an amount of material entering the interphase region. TMDSC [5,26–29,32,33] can provide accurate, qualitative and quantitative analytical expressions to measure the amount of material entering the interphase. For a partially miscible system the following equations apply

$$\Delta C_p = \Delta C_{p1} + \Delta C_{p2} + \Delta C_{pi} \tag{2}$$

$$\Delta C_{p1} = \omega_1 \Delta C_{p10} \tag{3}$$

$$\Delta C_{p2} = \omega_2 \Delta C_{p20} \tag{4}$$

where ΔC_{pi} is the increment of heat capacity of the interphase in its glass transition region and ω_1 and ω_2 are the weight fractions of polymer 1 and polymer 2, respectively, after mixing. The weight fraction of the two polymeric components can be easily calculated through the change in heat capacity both before and after mixing. Using TMDSC, the heat capacity can be measured using the following equation

$$\Delta C_p = \int_{T_i}^{T_f} \left[\frac{dC_p}{dT} \right] dT \tag{5}$$

where T_i and T_f are the initial and final temperatures, respectively, across the glass transition temperature.

While many studies [27–31,33] have investigated the interfacial properties and glass transition behaviour of various simple polymeric systems by TMDSC, few studies have attempted to investigate multi-component or other complex polymeric materials [5,32]. As the interfacial behavior between the component polymers in a blend largely controls the bulk polymer blend properties, an understanding of these interfaces as they develop during processing is of vital importance. To our knowledge, there is yet to be a qualitative or quantitative study on the relation of these parameters to the injection molding of complex rubber-modified thermoplastics such as PC/ASA. In this study, micro-thermal analysis was used to probe the phase morphology and determine T_g's of a PC/ASA blend after

processing at high injection times, packing pressures and melt temperatures. TMDSC was used to investigate the effect of processing on the interfacial properties of the styrene-acrylonitrile (SAN) and PC in the blend at both qualitative and quantitative level.

2. Experimental

2.1. Materials and sample preparation

A PC/ASA blend (Geloy XP4025) was supplied by GE Plastics, Australia. The composition of the material was determined using various spectroscopic methods and is listed in Table 1. AN and polybutylacrylate (PBA) rubber levels were determined by solution ^{1}H nuclear magnetic resonance (NMR) spectroscopy after separation of carbon black using high-speed, low temperature centrifugation in tetrahydrofuran (THF). PC and filler contents were calculated from thermogravimetric analysis (TGA) and bound acrylonitrile (AN) levels were determined according to ISO6402-2 method, by extraction with acetone followed by elemental analysis.

For convenient analysis, plastic pellets were compression molded into flat, workable samples using a temperature controlled 'Dake' compression molder and a hardened steel plaque mold ($190 \times 165 \times 1.5$ mm^3) at approximately 80 kPa pressure.

Injection molding was accomplished using a Ludgwig 'Engel' model ES 700/150 injection molding machine (Maschinefabrik Schwertberg-Austria) coupled with an MS (mild steel) plaque tool. Table 2 list the injection molding processing conditions that were used to produce each of the analysed strips. A total of 15 plaques per condition were manufactured using these settings. An initial purge period was used to dispose of any material remaining from previous runs.

2.2. Temperature-modulated differential scanning calorimetry (TMDSC)

TMDSC experiments were performed on a DSC 2920 from TA Instruments. TMDSC runs were both baseline and indium calibrated after an oxygen burn period of 60 min at 600 °C before each set of experiments for improved consistency and precision. Heat capacity calibration constants were determined using a sapphire calibrant, referenced against known literature values of aluminium oxide. Nominal 7 mg samples of pelleted PC/ASA as well as parts molded at ideal conditions, varying injection times and high pack pressures and melt temperatures were subjected to a modulated heating ramp of 3 °C/min at ±1 °C, every 60 s from 30 to 180 °C, with a helium purge gas rate of 50 ml/min. All experiments were done in duplicate for consistency. The curve of derivative heat capacity (dC_p/dT) was investigated to evaluate the effect of injection molding on the interface behaviour of PC and SAN. For semi-quantitative measurements, the development of interphases was analysed using PeakFit™ V4.05, assigning a linear two-point baseline before and after the glass transition regions of SAN and PC.

Table 1
Composition of PC/ASA

Component	Weight percent (%)
SAN	17.7
Unbound/bound AN	8.3/2.3
PC	11.7
PBA (*i*/*n*)[a]	29/22[b]
Gel content	21
Carbon black	9.6

[a] *i*/*n*—iso/normal.
[b] Refers to amount of polybutylacrylate (PBA) rubber and polymethylmethacrylate (PMMA) compatibilser.

2.3. Micro-thermal analysis

Micro-thermal analysis measurements were performed using the μTA 2990 Micro-Thermal Analyser (TA Instruments) with a thermal probe. As the probe scans across the sample surface two images are obtained; (1) surface topography; and (2) thermal conductivity (DC signal). The thermal diffusivity (AC signal) of the samples is similar to the conductivity images, since they are directly related to each other through density and heat capacity. A performance check was carried out on a semi-conductor silicon grid, which consists of raised SiO_2 squares with a 3 μm pitch, to determine whether the system was fully operational. The probe was temperature calibrated using polycarbonate and polyethylene of known T_g's and melting temperatures.

Analyses were performed directly on compression and injection molded plaques, which were sectioned and microtomed using a Leitz base sledge microtome into 40 μm slices and positioned onto a metallic sample stage using double-sided sticky tape. Scans were performed in DC mode at 55 °C. Samples were characterised at different locations using LTA, at a heating rate of 10 °C/sec. All images were scanned in a controlled environmental clean room laboratory. All T_g values were determined from the onset of the local thermal analysis sensor signal.

3. Results and discussion

3.1. Investigation of interphases and miscibility by TMDSC

3.1.1. Analysis of unprocessed phase-morphology

Conventional DSC heat flow and TMDSC determined heat capacity plots against temperature of the PC/ASA pellet are displayed in Figure 1. The heat flow trace clearly identifies the glass transition of SAN and PC at 105 and

Table 2
Injection molding parameters and plaque identification

Plaque no.	Injection time (s)	Packing press. (MPa)	Material temp. (°C)	Condition summary
1	2.7	5.5	260	Ideal
2	1.1	5.5	260	ITL
3	6.0	5.5	260	ITH
4	6.0	10	260	ITH, PPH
5	6.0	5.5	275	ITH, MTH

ITL–injection time low, ITH–injection time high, PPH–pack pressure high, MTH–melt temperature high.

141 °C respectively. However, it is difficult to draw conclusions about phases and boundaries with this data alone. Taking the plot of heat capacity (Fig. 1) and differentiating with respect to temperature dramatically increases quality of the information that can be interpreted from the plot. Fig. 2 displays the variation in dC_p/dT with temperature signal for the PC/ASA blend, prior to processing. Phase morphology is related to a transition temperature, which combines to form a transition thermogram [27]. Clearly, the morphology between SAN and PC is not a simple two-phase structure with sharp boundaries. The glass transition temperatures of SAN and PC are clearly visible at 109.7 and 143.3 °C, respectively. It is clear from the response of the dC_p/dT signal that SAN and PC are immiscible, as two distinct transition peaks are visible and separated by over 33 °C. This is due to the large differences in polarity between the polymers. However, neither curve displays a clear Gaussian response. Fig. 3 shows the baseline corrected and curve-fitted plot ($R^2 = 0.987$) of the same signal using the peak fit program. Both SAN and PC display small shoulders near their T_g. The peak at 105 °C represents the T_g of polymethylmethacrylate (PMMA), present in the blend as a compatibiliser. Its proximity to the SAN transition may signify a PMMA-SAN interphase, rather than a true PMMA T_g. The miscibility and phase behaviour of PMMA/SAN blends have been well documented [34–39] and can depend on such factors as AN content, copolymer composition and tacticity of PMMA. The shoulders at both 118.2 and 140.0 °C represent the presence of small PC-SAN interphases, which possess varying T_g values.

Studies of miscibility of SAN and PC have shown that partial miscibility may exist over a broad concentration of 23–70% AN in SAN [35,36,40], of which this material falls within. Keitz et al. [41] and Locati et al. [42] have reported that very little PC enters the SAN-rich phase, whereas a larger amount of SAN enters the PC-rich phase. Rubber-modified PC/ASA is a more complex system than a two-phase, PC/SAN blend that contains an amount of bound and unbound poybutylacrylate as well as fillers and additives. Previous studies [43] have stated that there is no contribution to miscibility from the rubber phase. Rather, a surface energy effect may result where the rubber phase may adhere to the PC-rich phase.

3.1.2. Interface development during processing

A comparison of responses to dC_p/dT for both pelleted and ideally injection molded PC/ASA is displayed in Fig. 4. The act of processing clearly shows an increase in the dC_p/dT signal between the two glass transition temperatures, indicating that the concentration and thickness of the interphase have increased. The increment of heat capacity at each corresponding T_g has also decreased. This is attributed to portions of both PC and SAN entering the interfacial regions [31,33]. It should also be noted that the T_g values of both SAN and PC have shifted, most noticeably the latter that has dropped by over 3 °C. In addition, the peak associated with the T_g of PC shows considerable broadening, indicating interaction with SAN. This is in contrast

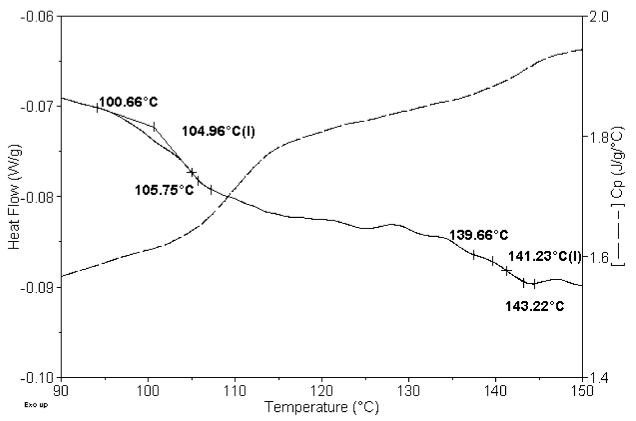

Fig. 1. A comparison of conventional DSC heat flow and TMDSC heat capacity (C_p) signals against temperature for unprocessed PC/ASA.

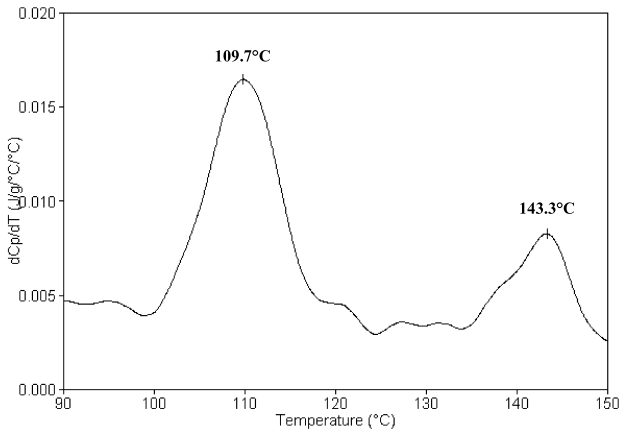

Fig. 2. Plot of dC_p/dT against temperature for unprocessed PC/ASA.

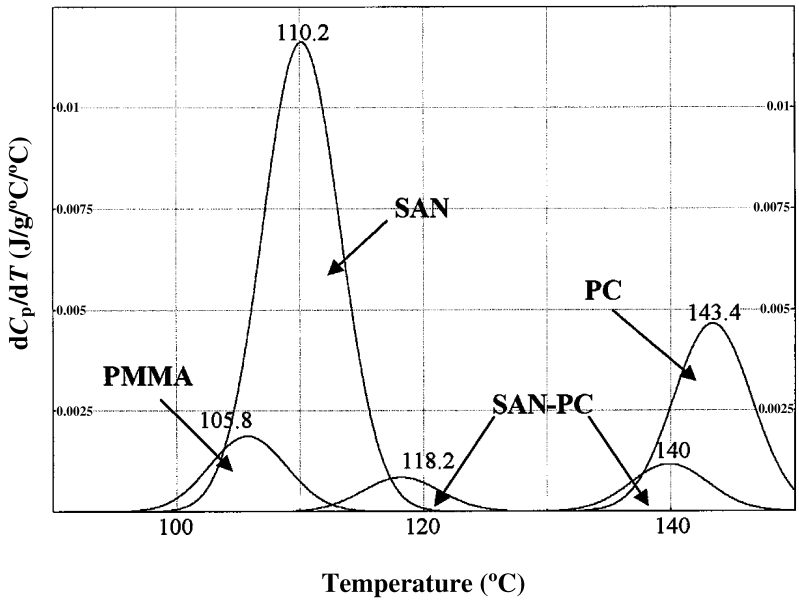

Fig. 3. Peak fitted plot of dC_p/dT against temperature for unprocessed PC/ASA with phase identification.

with observations by Keitz et al. [41] and Locati et al. [42]. It is generally noted [43], that a lower T_g polymer will inter-diffuse more easily into a phase with a higher T_g. However, if the high T_g component exhibits low molecular weight as does PC in this study, its inter-diffusion is readily facilitated, particularly at high temperatures and pressures as seen in processing. Regardless of the method used, the T_g of the polymer depends on its previous history, experimental time scale and other factors that influence its intermolecular forces. T_g is very sensitive to disruption of local structure resulting from processing. Thus the existence of (a) single or sharp, (b) single and broad, (c) double and shifted and (d) double and non-shifted T_g reveals the macroscopic character and interfacial behaviour of such blend systems.

The baseline-corrected, peak-fitted dC_p/dT response ($R^2 = 0.993$) of the injection molded specimen is shown in Fig. 5. The increase in size of the SAN-PC interphase is very apparent, most noticeably at 133.5 °C that suggests the interface is PC-rich. Expanding on this to include variations in pack pressures and melt temperatures (Fig. 6), where plaque 1 is compared to plaques 4 and 5. Injection molding, regardless of processing conditions, follows a similar pattern to that seen in the ideal case, though it is difficult to differentiate this on a qualitative basis using purely a visual interpretation.

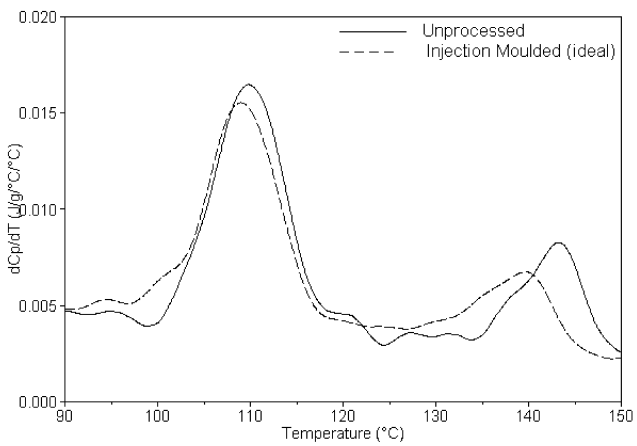

Fig. 4. Plot of dC_p/dT against temperature for unprocessed PC/ASA and ideally injection molded (plaque 1) PC/ASA.

3.1.3. Quantitative analysis of interphase composition

Eqs. (1)–(5) describe how the amount of SAN and PC in the interphase can be estimated, calculated through the 'missing' amount of the ΔC_p of each transition. Table 3 lists the weight percent of both the SAN and PC phase entering the SAN-PC interphase region during injection molding, using compression molded material as the base reference (ie. physical mixture). The fact that this material is an inherently complex system makes this calculation semi-quantitative, as the interference and contribution from PMMA, rubber as well as additives is unknown. In the ideal case, the amount of PC entering the interphase is around 20%. The ΔC_p of the SAN transition is found to increase by

Table 3
Weight percent of SAN and PC content entering the interphase during injection molding

Plaque no.	Weight percent (%) in the interphase	
	SAN	**PC**
1	−2.4[a]	19.9
2	5.5	27.6
3	26.4	48.6
4	18.9	34.3
5	22.3	41.7

[a] An increase in the SAN ΔC_p peak.

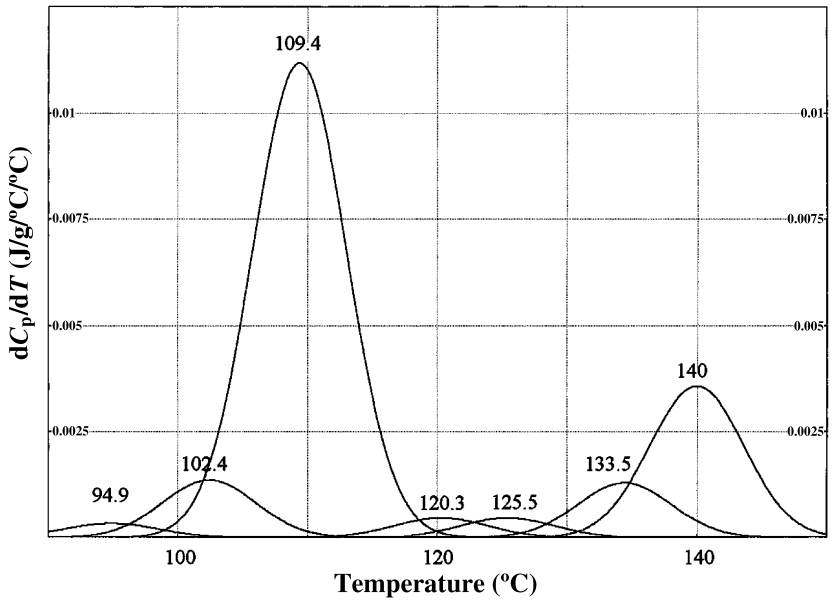

Fig. 5. Peak fitted plot of dC_p/dT against temperature for plaque 1.

2.4%, which may signify an increase in the PMMA-SAN interface.

Under extremes of processing, the SAN content in the interphase is considerably higher, most noticeably at long cycle times and high melt temperature and pack pressure where it ranges from 22.3 to 26.4%. At short cycle times however, the drop of the SAN transition more closely resembles that of the ideal case with 5.5% entering the interface. Similarly with SAN, the amount of PC entering the interphase increases at long injection times and high melt temperature and pack pressure, with values ranging from 34.3 to 48.6%, suggesting that the amount of PC entering the interphase is greater than SAN over all processing conditions. This is due to a combination of high shear and temperature as well as PC's low molecular weight and shear-thinning properties.

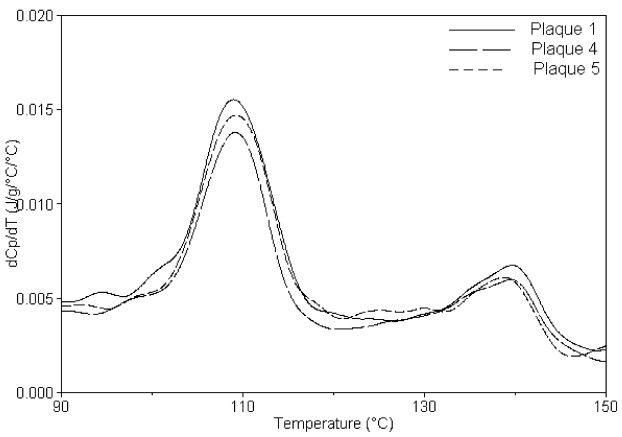

Fig. 6. Plot of dC_p/dT against temperature for plaques 1, 4 and 5.

3.2. Morphology and interphase development with injection molding by micro-thermal analysis

3.2.1. Analysis of relative thermal conductivity

A comparison of topography and relative thermal conductivity scans of a microtomed section of compression molded PC/ASA and plaque 1 (ideal) is shown in Fig. 7A and B, respectively. Both topography and thermal images are examined and shown, as variations in heat flow may also be the result of large changes in topography. Whilst the probe is in a valley it is primarily surrounded by the sample and when on a peak, it is surrounded by air. Thus, the thermal homogeneity of the sample will vary the image contrast and the measured thermal conductivity increases and decreases, respectively, [12]. In Fig. 7, similarities exist between topography and their corresponding thermal profiles, most noticeable in regions of extreme low conductivity, seen as black spots. Another consideration is that since the sample has been sheared during microtoming, topography itself may provide hints on the morphology of the sample. Various phases within the plastic deform under shear in different ways and will relax to varying amounts, manifesting itself in the topography image [1].

As with our previous work [6], thermal images are consistent with the structural model of rubber-modified thermoplastics, consisting of varying sizes of discrete oval and circular-shaped rubber zones of lower conductivity embedded in a continuous matrix of higher conductivity. Individual rubber particles cannot be seen although clusters and grafted zones of the gel are clearly visible throughout the images. In addition, at the interface between the rubber zones and the matrix, the relative conductivity is higher compared with the particles themselves, indicating the coexistence of phases and partial mixing.

It is clear from the injection molded specimen (Fig. 7B)

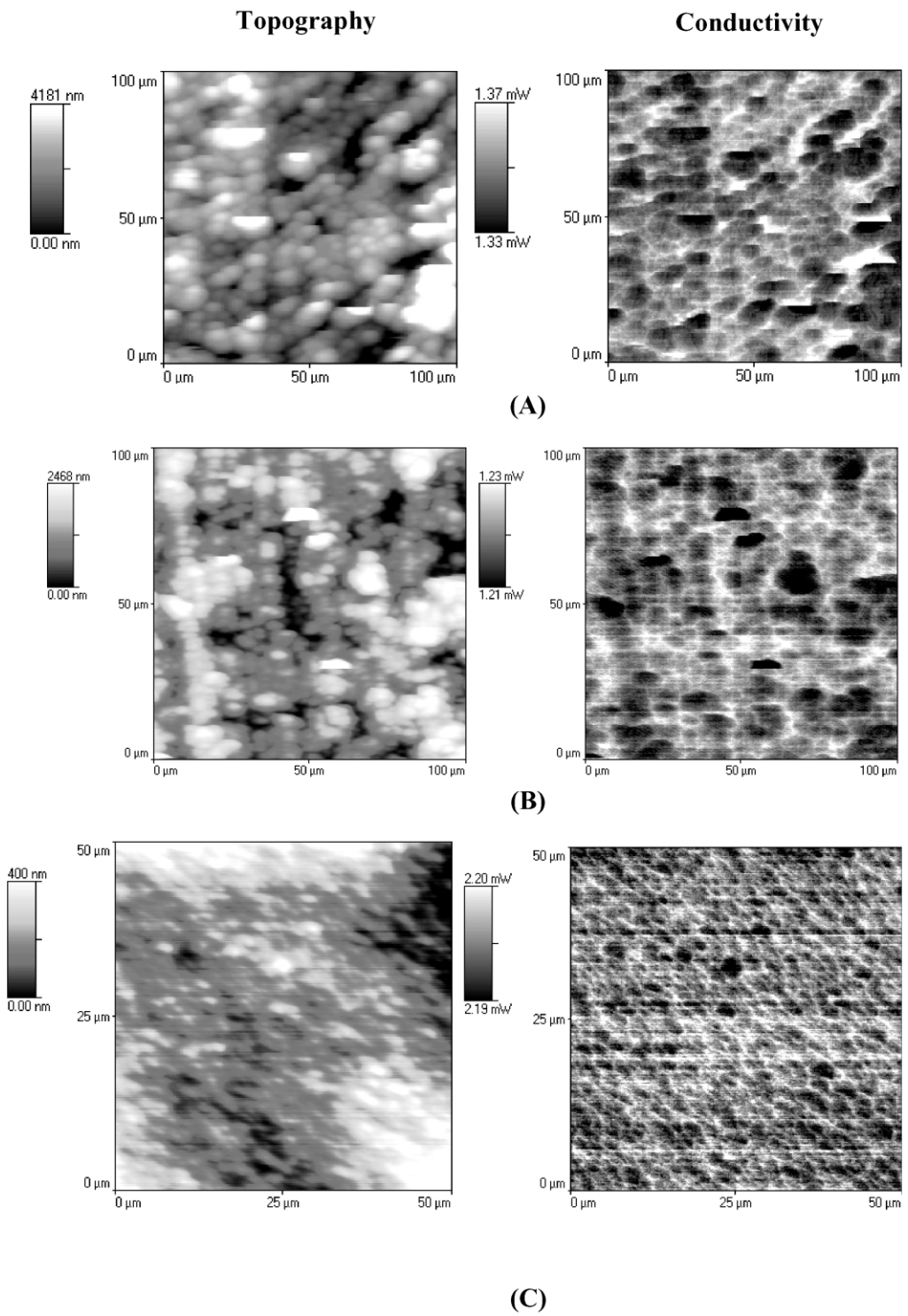

Fig. 7. Topography and relative thermal conductivity images of PC/ASA microtomed sections of (A) compression molded and (B) injection molded (plaque 1) (C) compression molded but micro TA sample preparation method different.

that the boundaries between clusters of lower conductivity have partially broken down and a degree of phase mixing has occurred. As the amount of interphases (intermediate regions of conductivity) has increased during processing, the mobility within these regions will be increasingly restricted. Therefore, the glass transition temperatures are likely to be affected in these regions. While these observations reveal a subtle change in morphology in the bulk-core region, the original unprocessed, multi-phase morphology is still visible. However, sections when cut to approximately 1–5 μm thickness, adhered to conductive carbon tabs and placed directly on the sample stage for

imaging show some clear differences in images as seen in Fig. 7C. In the figure, little similarities exist between topography and thermal profiles and thus influences from the height of the sample are only very small and are limited to regions of extreme low conductivity, seen as black spots. Thermal images are still consistent with the structural model of rubber-modified thermoplastics, consisting of varying sizes of discrete oval and circular-shaped rubber zones of lower conductivity embedded in a continuous matrix of higher conductivity, however, clarity is dramatically improved.

Figs. 8A–D display the relative thermal conductivity scans of the bulk-core morphology of plaques produced at various injection times, pack pressures and melt temperatures. Figs. 8A–B display the bulk morphology of parts molded at a low (plaque 2) and high injection time (plaque 3) respectively. Differences can be seen when contrasting the two images. Plaque 2 displays a similar morphology to plaque 1, showing clusters of low conductivity embedded in a higher conductivity matrix as well as partial amounts of phase mixing. The morphology of the part molded with a higher injection time reveals a greater amount of mixing than does plaque 1 or 2. The longer cycle time involved in the production of this plaque has obviously altered the core morphology, allowing time for increased phase mixing.

The effects of taking a higher injection time and adding both a higher packing pressure (plaque 4) and melt temperature (plaque 5) on the bulk morphology can be seen in Figs. 8C and D. An increase in pack pressure (Fig. 8C) results in smaller particles and further densification of the morphology, agglomeration and deformation of lower conductivity particles. Similarly, an increase in melt temperature up to 275 °C (Fig. 8D) raises the amount of phase mixing and agglomeration dramatically, as higher temperatures favour thermal diffusion and the formation of interphases.

3.2.2. Localised thermal analysis (LTA)

Spot thermal analysis by LTA provided consistent results, noting differences between bulk glass transition temperatures of injection molded plaques with those obtained from the original unprocessed material. An example is shown in Fig. 9, which displays both the LTA of plaque 1 and the compression molded sheet. The curves of the unprocessed material confirm the presence of both SAN and PC, with glass transition temperatures determined in the range of 100–124 °C and 135–159 °C, respectively, and is in agreement with TMDSC results. Furthermore, the thermal inter-diffusion under high shear and pressure, as seen in Fig. 4, complements both LTA and relative thermal conductivity data from Fig. 9. Low temperature rubber transitions cannot be seen, as without a cold stage they are beyond the detection limit of the probe. As mentioned previously, at the interface between the rubber zones and the matrix, the relative conductivity is higher compared to the particles themselves. This explains why ranges of

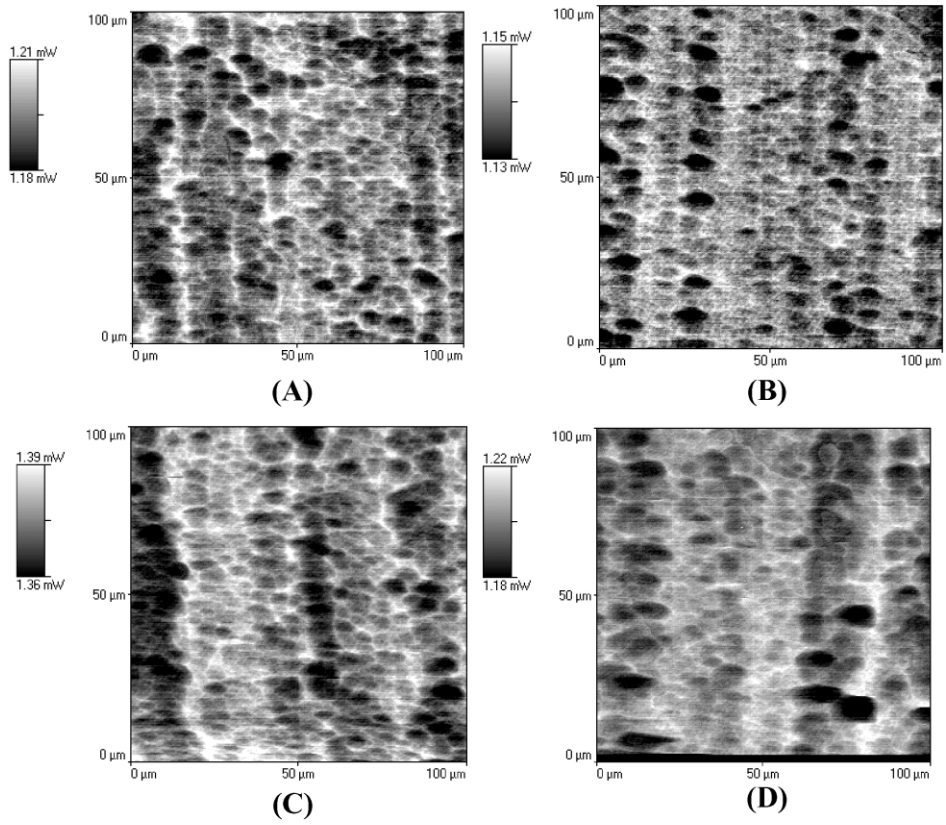

Fig. 8. Relative thermal conductivity scans of microtomed sections of (A) plaque 1, (B) plaque 2, (C) plaque 3 and (D) plaque 4.

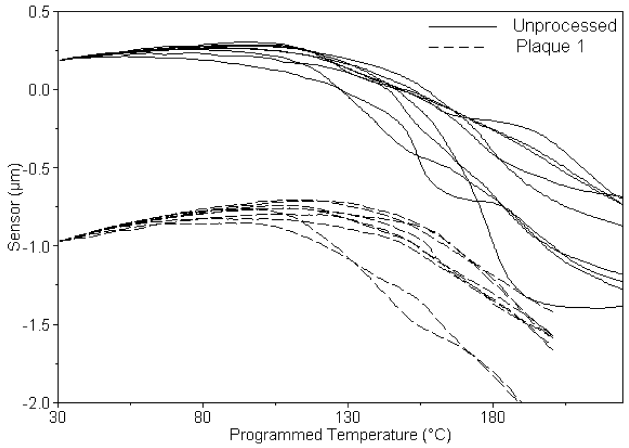

Fig. 9. LTA spot analysis in nine locations on both unprocessed and ideally injection molded (plaque 1) PC/ASA.

glass transitions are calculated from LTA, as within these confined regions, mobility of the phase is greatly restricted.

The nine LTA traces from plaque 1 reveal the presence of SAN, PC as well as the formation of interphases as suggested by images of thermal conductivity and TMDSC results. T_gs temperatures have increased in these regions and only one transition is detectable. The width/breadth of this transition varies, indicating the coalescence of SAN and PC phases to different extents. LTA-determined T_g's of unprocessed and processed sections of the imaged specimens are listed in Table 4. On more severely molded plaques, marked differences in the T_g's are clearly visible and are consistent across all test pieces. This phenomenon is more clearly noticed at high injection times and pack pressures where there is a clear increase in T_g values and in some cases, one broad transition.

Depending on the injection molding conditions, various phases may co-exist on the surface or sub-surface of the molded part. Therefore, T_gs will be governed by the weight fraction of each phase/component present in that particular location and can be expressed by the following equations [44]:

$$T_g = \omega_1 T_{g1} + \omega_2 T_{g2} \quad (6)$$

$$\omega_1 + \omega_2 = 1 \quad (7)$$

where ω is the weight fraction of the respective phase. In addition, as LTA analysis is a highly localised technique, high values of T_g temperatures are often seen and signify a restriction in mobility at the point of analysis. Over such small scales, the presence of rubber particles in the blend, both bound and unbound, will affect the mobility of matrix chain segments that lay within an 'entanglement' or 'entrapped' zone [1]. This will however, be more obvious on the surface of plaques [6], where agglomeration and skin-layers can form.

4. Conclusions

TMDSC qualitatively and quantitatively characterized the multi-phase morphology of a PC/ASA thermoplastic and its interfacial properties both before and after injection molding. The morphology between SAN and PC in rubber-modified PC/ASA is not a simple two-phase structure with sharp boundaries.

Thermal conductivity images of processed parts, most noticeably those manufactured at high injection time, pack pressure and material temperature, revealed a densely packed bulk morphology with evidence of phase mixing and a significant amount of particle agglomeration. LTA analysis confirmed the formation of SAN-PC interphases.

The derivative heat capacity data from TMDSC for unprocessed material revealed the presence of a small PC-SAN interphase, explaining why a range of glass transition temperatures were calculated from LTA curves.

A comparison of responses to the curve of derivative heat capacity for both pelleted and ideally injection molded specimens indicated that the concentration and thickness of the interface increased due to thermal inter-diffusion under high shear and pressure that occurs during processing. These results are in line with the relative thermal conductivity and

Table 4
LTA-determined T_g for microtomed samples of compression and injection molded PC/ASA

Sample	T_g (°C) at various locations (microtomed)								
	1	2	3	4	5	6	7	8	9
Unprocessed	118.6	106.4	114.5	109.8	104.1	100.0	124.1	107.2	104.6
					145.0	159.2			135.0
1	114.0	115.9	123.7	111.7	122.4	121.8	126.0	107.8	115.7
	127.5			140.3	145.7	140.8		137.8	
2	91.5	82.5	159.7	–	115.0	86.9	111.7	–	100.6
		147.0			169.8	119.5			
3	105.8	–	153.0	149.2	122.7	–	117.0	119.7	144.7
4	83.4	119.7	93.9	156.4	80.6	104.4	127.4	159.5	153.8
	134.2								
5	–	156.1	156.4	114.6	139.3	119.4	124.9	154.8	140.2
				162.0	158.8		143.2	174.1	167.9

glass transition data obtained by micro-thermal analysis/LTA.

Quantitative analysis of the interface formed during injection molding showed that the amount of PC entering the interphase was greater than SAN over all processing conditions, particularly at high melt temperature, high pack pressure and long cycle times. The maximum weight percent of PC entering the interphase varies up to 48.6%, while that for SAN is 26.4%. This study thus demonstrates that a combination of TMDSC and micro-thermal analysis/LTA adds another dimension to the interface analysis of in situ developed morphology of immiscible systems.

Acknowledgements

The authors are thankful to the Australian Research Council (ARC) and Schefenacker-Australia for support of this work through the collaborative grant scheme.

References

[1] Edwards SA, Provatas M, Roy Choudhury N, Tran ND, Dutta NK. Visualisation and characterisation of bulk and surface morphology by micro thermal analysis and atomic force microscopy. Marcel Dekker; 2003 in press.
[2] Hatakeyama T, Liu Z. Handbook of thermal analysis. Wiley; 1998.
[3] Bair HE, Twombly B. Proc 54th Annu Tech Conf Soc Plast Engng 1996;2449–53.
[4] Ginic-Markovic M, Roy Choudhury N, Dimopolous M, Willams DRG, Matison JG. Thermochim Acta 1998;316(1):87–95.
[5] Song M, Hourston DJ, Reading M, Pollock HM, Hammiche A. J Therm Anal Cald 1999;56(3):991–1004.
[6] Provatas M, Edwards SA, Roy Choudhury N. Thermochim Acta 2002; 392–393:339–55.
[7] Edwards SA, Roy Choudhury N. Polym Engng Sci 2003; in press.
[8] Song M, Hourston DJ, Grandy DB, Reading M. J Appl Polym Sci 2001;81(9):2136–41.
[9] Price DM, Reading M, Lever TJ. J Therm Anal Cald 1999;56(2): 673–9.
[10] Häßler R, zur Mühlen E. Thermochim Acta 2000;361(1–2):113–20.
[11] Hammiche A, Pollock HM, Reading M, Claybourn M, Turner PH, Jewkes K. Appl Spectrosc 1999;53(7):810–5.
[12] Royall PG, Kett VL, Andrews CS, Craig DQM. J Phys Chem B 2001; 105(29):7021–6.
[13] Reading M, Price DM, Grandy DB, Smith RM, Bozec L, Conroy M, Hammiche A, Pollock HM. Macromol Symp 2001;167:45–62.
[14] Moon I, Androsch R, Chen W, Wunderlich B. J Therm Anal Cald 2000;59(1–2):187–203.
[15] Hammiche A, Reading M, Pollock M, Song M, Hourston DJ. Rev Sci Instrum 1996;67(12):4268–74.
[16] Price DM, Reading M, Hammiche A, Pollock HM. Int J Pharm 1999; 192(1):85–96.
[17] Royall PG, Craig DQM, Price DM, Reading M, Lever TJ. Int J Pharm 1999;192(1):97–103.
[18] Feng J, Weng LT, Chang CM, Xie J, Li L. Polymer 2001;42(5): 2259–62.
[19] Kuutti L, Peltonen J, Myllärinen P, Teleman O, Forssell P. Carbohydr Polym 1998;37(1):7–12.
[20] Xie W, Liu J, Lee CWM, Pan WP. Thermochim Acta 2001;367–368: 135–42.
[21] Edwards SA, Roy Choudhury N, Provatas M, Matisons J. J Appl Polym Sci 2003;87(5):774–86.
[22] Zipper MD, Simon GP, Tant MR, Small GD, Stackand GM, Hill AJ. Polym Int 1995;36:127.
[23] Zipper MD, Simon GP, Flaris V, Campbell JA, Hill AJ. Mater Sci Forum 1995;189–190:167.
[24] Reading M, Elliot D, Hill VL. Proc Nineth ICT Meeting, Hatfield, UK, 1992. J Therm Anal 1993;40:949.
[25] Gill PS, Saurburn SR, Reading M. Proc. 9th ICT Meeting, Hatfield, UK, 1992. J Therm Anal 1993;40:931.
[26] Jiang Z, Imrie CT, Hutchinson JM. Thermochim Acta 2002;387(1): 75–93.
[27] Hourston DJ, Song M, Hammiche A, Pollock HM, Reading M. Polymer 1997;38(1):1–7.
[28] Song M, Hammiche A, Pollock HM, Hourston DJ, Reading M. Polymer 1995;36(17):3313–6.
[29] Song M, Pollock HM, Hammiche A, Hourston DJ, Reading M. Polymer 1997;38(3):503–7.
[30] Donth EJ. Relaxation and thermodynamics in polymers. Berlin: Academie; 1992.
[31] Kang HS, MacKnight WJ, Karasz FE. Polym Prepr 1987;28:134.
[32] Hourston DJ, Song M. J Appl Polym Sci 2000;76(12):1791–8.
[33] Fried JR. Thesis, University of Massachusetts; 1976.
[34] Greco R, Sorrentino A. Adv Polym Technol 1994;13(4):249–58.
[35] Paul DR, Bucknall CB. Polymer blends. Formulation, vol. 1. New York: Wiley; 2000.
[36] Fowler ME, Barlow JW, Paul DR. Polymer 1987;28(7):1177–84.
[37] Dean BD. J Appl Polym Sci 1985;30(10):4193–6.
[38] Cameron N, Cowie JMG, Ferguson R, Gomez Ribelles JL, Mas Estelles J. Eur Polym J 2002;38(3):297–605.
[39] Hsu WP. J Appl Polym Sci 1999;74(12):2894–9.
[40] Mendelson RA. J Appl Polym Sci 1987;22:2739.
[41] Keitz JD, Barlow JW. Polymer 1984;25:487.
[42] Locati G, Giuliani G. Rheology. Proceddings of Eighth International Congress on Rheology, vol. 3. New York: Plenum Press; 1980. p. 205.
[43] Bertilsson HE, Kubat J, Ribarits E. Plast Rubber Compos Process Appl 1993;19(4):211–20.
[44] Brandch R, Bar G. Langmuir 1997;13:6349.